Research and Application of Ankle Morphological Changes and Classification

Chunqiang Zhang [1*], Xiaomin Ji [1], Yanmin Xue [1] and Gang Hu[1]

[1]Xi'an University of Technology, Xi'an, Shaanxi, 710054, China

Abstract. Because of the motion of ankle joint, the surface morphological changes. The relevant products including ankle brace, ankle boot, etc. with both important protective effect on ankle and comfort should be designed to match the ankle varies states. The samples data with 15° plantar flexion, 40° dorsiflexion and neutral position of lower limbs(N=105) were scanned. This study analyzed the feature of the ankle morphological changes and divided it into four parts: anterolateral (I), posterolateral (II), posteromedial (III) and anteromedial (IV). The anterior and posterior parts had large contraction and expansion during plantar flexion and dorsiflexion motions. The medial and lateral parts of ankle shape were asymmetric, but had equal skin areas. Therefore, the area of the entire ankle surface remained almost the same when morphological changes. We unified the data of the models and measured the distances of characteristic points. According to the main dimensions, the ankles were classified into 17 groups. The rigid brace design was taken as an example to fit mass ankles. It showed a great statistical comfort degree in total by the user experience and evaluation. The method combining with features of ankle morphological changes and shape classification was proved to be effective for the ankle related products design to fit mass ankles.

1 Introduction

The ankle joint complex bears a force of approximately five times body weight during stance in normal walking, and up to thirteen times body weight during activities such as running[1]. In sports, ankle ligament injury is occurred frequently[2]. Therefore, it is very important for the design of ankle related products to be of protectiveness and comfort. At present, for the design of many products and the purpose of obtaining the parameters matching with human body, images technology is used to obtain the data of the relevant parts in human body. The shapes classification is very effective as the main reference method of product design. Various kinds of images technology are widely used in different research fields. 3D internal images of a patient body, X-rays, computed-tomography, (CT) scanners, Ultrasound and Magnetic resonance imaging (MRI) are commonly used to measure body shape and size[3]. For example, the morphometry of the ankle joint including the radius, arc length, width of the trochlea tali and the tibial was evaluated by CT scanning database[4]. For the product design based on human body dimensions, Yu et al.[5] measured and analyzed the ear canal of human body through the technology of CT scanning and digital measurement, so as to complete the style design of hearing aid and noise reduction earplug. Harih et al.[6] made statistical analysis on the three-dimensional hand shape in the grip state through the MRI technology, and established the design method of reverse tool handle

shape through the static digital hand model, which greatly improved the user's comfort during operation. With the advent of 3D scanners, which are safe and convenient to use to measure a person's body shape, size, texture, colour and skin-surface area accurately, a new application is emerging, i.e. 3D scanning has a high capability of capturing 3D measurement[7]. Ji et al.[8] obtained the data of concha cavity by 3D scanning technology, and classified the shapes of concha cavity, which was used in the earphone modeling design. Many studies have reported the design of human foot related products. Using 3D foot-scan database for statistical foot shape analysis that can be applied to improve the comfort degrees of insole and footwear[9-13]. However, for the ankle, most studies are focus on the ankle joint including kinematics, biomechanics, etc. But few studies reported the external shape of ankle. The relevant products with both important protective effect on ankle and comfort, such as ankle brace, ankle boot, short boot, and long boot, which involve the shape and size of the ankle when they are designed. In this study, 3D scanning data is used to obtain the characteristic points and distances of ankle. The features of ankle morphological changes are analyzed and the key characteristic distance clustering method is used to classify ankle shape. The rigid brace design will be taken as an example to fit mass ankles.

---

*Corresponding author's e-mail: 12130137@qq.com

2 Materials and Methods

2.1 Participants and acquisition of 3D scanning data

The morphology of ankle involved the foot and lower leg. The data of lower limber with 15° plantar flexion (Pf), 40° dorsiflexion (Df) and standing state (St) of lower limbs from participants (N=105, 52 males and 53 females) were scanned. The lower limber surface point cloud data was obtained using the Creaform Go!SCAN 3D scanner with an accuracy of 0.1mm. The missing point were repaired by ImageWare software platform. Approximate data can be obtained for the left lower limb by mirroring.

2.2 Characteristic points and distances

From the scanning data, it can be found that there are two main characteristic points for the morphological changes of ankle in the foot part. One is the instep and the other is the heel. Point A is defined as the starting point of morphological change of instep, while point B is defined as the starting point of morphological change of heel.

The coordinates of the two points are A and B, a plane that passes through these two points and parallels the coronal axis of the ankle. The points less than the given threshold (1mm) from the plane can be obtained. These points constituted a closed curve is of girth as the dividing line between the foot and ankle, denoted as line FL. The morphological changes of ankle in the lower leg part are mainly under the minimum girth (LL). Point E is defined as the endpoint on the anterior side, while point F as the endpoint on the posterior side. Point C is defined as the protrusion point of the medial malleolus of tibia, point D as the protrusion point of the lateral malleolus of fibula, and point O as the midpoint of line CD. There is a plane that goes through the points C and D and is perpendicular to the line AB. The plane intersects with line AB and girth FL at points P, G, and J. Another plane is perpendicular to the line EF, and intersects with line EF and girth LL at points Q, H, and K respectively. Points H and K represent the inside and outside width position characteristic points of girth LL, and points G and J respectively represent that of girth FL. Figure 1 shows the characteristic points and lines of ankle surface. Table 1 depicts statistical analysis of characteristic distances for 105 participants, while Table 2 describes statistical analysis for males and females.
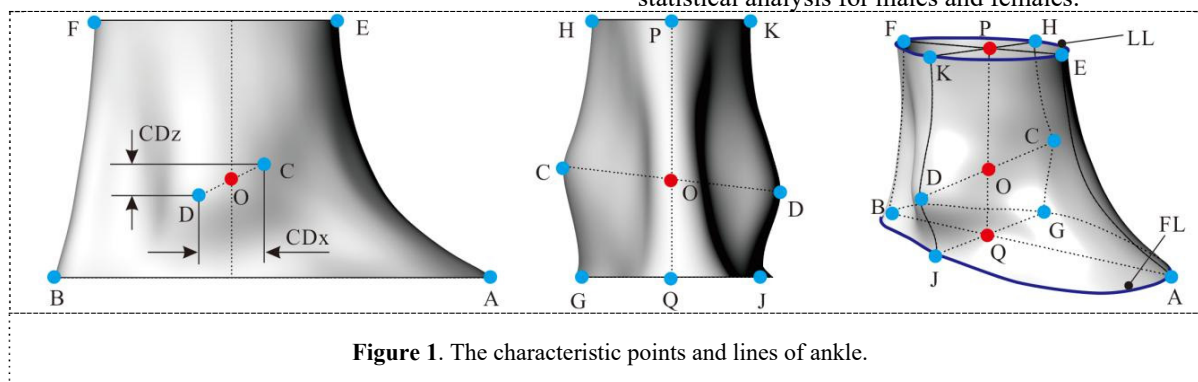

Figure 1. The characteristic points and lines of ankle.

Table 1. Describe statistical analysis for 105 participants (mm).

	AB	GJ	FL	EF	HK	LL	CD	CDz	CDx	PQ	OQ	BQ
Mean	125.3	56.6	303.9	76.7	62.4	209.8	70.0	11.2	10.1	67.6	25.8	55.3
Max.	140.4	73.9	342.4	94.3	79.5	267.8	81.7	22.5	18.8	83.8	36.8	67.5
Min.	106.1	47.1	257.7	66.7	52.3	182.7	58.4	2.8	5.0	49.5	18.3	42.0
SD	8.59	4.78	19.51	5.15	4.65	15.45	4.85	4.23	2.61	8.91	3.76	5.05

Table 2. Describe statistical analysis for males and females (mm).

		AB	GJ	FL	EF	HK	LL	CD	CDz	CDx	PQ	OQ	BQ
Mean	Male	130.9	58.0	317.2	78.8	65.1	215.3	73.5	12.7	10.8	73.9	27.5	57.7
	Female	119.9	55.2	291.0	74.7	59.8	204.3	66.6	9.7	9.4	61.5	24.2	52.9
Max.	Male	140.4	73.9	342.4	94.3	79.5	267.8	81.7	22.5	17.6	83.8	36.8	67.5
	Female	135.5	64.5	330.5	85.8	70.1	229.4	76.1	21.1	18.8	75.4	31.4	63.3
Min.	Male	113.5	47.1	281.0	69.2	59.2	182.7	64.9	4.6	6.4	55.5	19.5	49.4
	Female	106.1	49.1	257.7	66.7	52.3	187.1	58.4	2.8	5.0	49.5	18.3	42.0
SD	Male	6.46	5.56	13.93	5.70	4.06	18.05	3.29	3.92	2.40	6.50	3.70	3.95
	Female	6.82	3.41	14.99	3.61	3.63	9.83	3.47	4.03	2.63	6.37	3.03	4.92

3 Morphological changes and classification

3.1 The morphological division and the features of dynamic change

In order to discuss the characteristics of change of ankle during plantar flexion and dorsiflexion, the morphology is divided into four parts. The part AEKJ is the anterolateral area, denoted as I, the part JKFB as the posterolateral area II, BFHG as the posteromedial area III, and GHEA as the anteromedial area IV. The change of morphology is mainly attributed to the ankle caused by ankle joint and the contraction of relevant muscles in foot and leg. From the appearance, the skin of the ankle expands or contracts, the area changes and the wrapping morphology changes. The four parts change dramatically when the ankle joint extends or flexes.

Table 3 lists the mean areas of the four parts (I, II, III and IV) in three states. Part I (AEKJ) contracts when dorsiflexion and expands when plantar flexion. The ratios of the area in dorsiflexion state ($6258mm^2$) and plantar flexion state ($7675mm^2$) to standing state ($6422mm^2$) are 0.97 and 1.20 respectively. The ratio of

area from dorsiflexion to plantar flexion is 0.82. Namely, the plantar flexion area is 1.23 times as large as the dorsiflexion. Part II (JKFB) expands when dorsiflexion and contracts when plantar flexion. The ratios of the area in dorsiflexion state ($4370mm^2$) and plantar flexion state ($3040mm^2$) to standing state ($3708mm^2$) are 1.18 and 0.82. The ratio of area from dorsiflexion to plantar flexion is 1.44. Part III (BFHG) is the same as Area II, that is, it expands when dorsiflexion and contracts when plantar flexion. The ratios of the area in dorsiflexion state ($6224mm^2$) and plantar flexion state ($4012mm^2$) to standing state ($5883mm^2$) are 1.06 and 0.68. The ratio of area from dorsiflexion to plantar flexion is 1.55. Part IV (GHEA) is the same as Area I, that is, it contracts when dorsiflexion and expands when plantar flexion. The ratios of the area in dorsiflexion state ($4056mm^2$) and plantar flexion state ($6365mm^2$) to standing state ($5122mm^2$) are 0.79 and 1.24. Namely, the plantar flexion area is 1.57 times as large as the dorsiflexion.

The anterior and posterior parts had large contraction and expansion during plantar flexion and dorsiflexion motions. The medial and lateral parts of ankle shape were asymmetric, but had equal skin areas. Therefore, the area of the entire ankle surface remained almost the same when morphological changes.
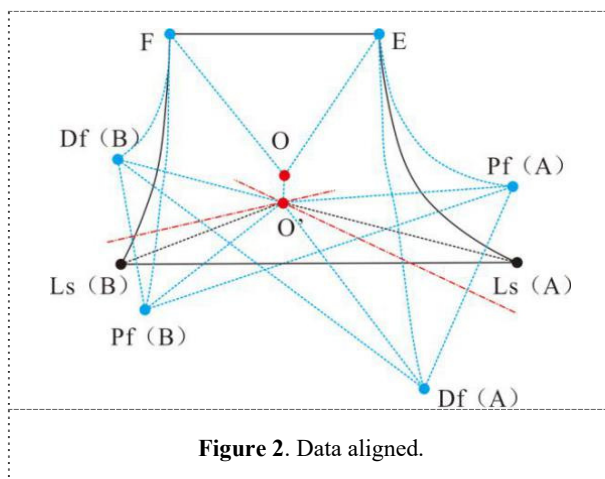
Table 3. Mean areas of the four parts (mm^2).

	I（AEKJ）	II（JKFB）	III（BFHG）	IV（GHEA）	Total
St(S)	6422	3708	5883	5122	21307
Dt(S)	6258	4370	6224	4056	20917
Pt(S)	7675	3040	4012	6365	21153

3.2 Data aligned and standard model

Because the range of motion of ankle joint changes, even in the same statement, the data should be aligned to classify the ankle shape. Ankle plantar flexion and dorsiflexion are the rotation movement of the foot on the sagittal plane with a center point. The point Df(A) is the point A in dorsiflexion of ankle and point Pf(A) as the plantar flexion, the same of points Df(B) and Pf(B). The intersection point O' of the perpendicular bisector of line Df(A)Pf(A) and Df(B)Pf(B) is the the rotation center of the foot (figure 2). With O' as the center, rotate the data of the girth FL parallel to the plane of the girth LL, mark characteristic point A as Ls(A) and characteristic point B as Ls(B) in this state. For all 105 samples, we use the same method so as to unify the dynamic morphological model of ankle. The standard model can be constructed.

Figure 2. Data aligned.

3.3 Shape classification

Pearson's test method was used to detect the main dimensions of ankle in pairs. The results showed that there were significant linear correlation between AB, GJ, and FL ($r > 0.90$), significant linear correlation between EF, HK, and LL ($r > 0.90$), and significant linear correlation between OP and PQ ($r > 0.90$). Points C and D are two prominent points of ankle shape, which should be classified as characteristics, but there is a certain linear correlation between CD and AB ($r = 0.494$), and between CD and EF ($r = 0.452$). At the same time, we

test the relationship between QB and AB (r = 0.631) which shows that there is also a certain linear correlation. This means the position of point O on the x-axis is related to the distance of AB. Based on the above discussion, we classify the ankle height PQ (included OP), leg distance EF (included HK and LL) and foot distance AB (included GJ and FL) as three types, and then separately discuss the location of C and D (position of point O) and the distribution of dimension CD . According to the ankle height PQ, it can be divided into three type ranges of I, II, and III (49.5mm ≤ I ≤ 60.9mm, 60.9mm < II ≤ 72.4mm, and 72.4mm < III ≤ 83.8mm), representing the types of ankle height. According to the length AB, it can be divided into S, M, and L (106.1mm ≤ S ≤ 117.5mm, 117.5mm < M ≤ 129.0mm, and 129.0mm < L ≤140.4mm), representing the three types divided by the foot size, and with the length EF, it can be divided into ①, ②, and ③ (66.7mm ≤ ① ≤ 75.9mm, 75.9mm < ② ≤ 85.1mm, and 85.1mm < ③ ≤ 94.3mm), representing three types divided by leg size.

To display the classification form more intuitively, all points are converted to the coordinate system with B as the origin (0, 0, 0), and BA direction is x' axis. The distribution of point F(figure. 3) on the boundary of types I, II, and III is obtained by the following methods: (1) H_1 (0, 0, 60.9), H_2 (0, 0, 72.4), and H_3 (0, 0, 83.8) are taken on the z-axis, and the horizontal lines h_1, h_2 and h_3 are made respectively. (2) Draw lines from characteristic point B to all characteristic points F. (3) Find lines BF with minimum angle from positive z-axes in each group of I, II, and III. (4) Extend BF to intersect with h_1, h_2 and h_3. The intersecting points F_1, F_2 and F_3 would be the boundary location of each group, as shown in the figure. For point A, taking A_1, A_2, and A_3 respectively according to the upper limit of three ranges of AB, there are BA_1 = 117.5mm, BA_2 = 129.0mm, BA_3 = 140.4mm. Point E is distributed on h_1, h_2 and h_3 according to the height types. At the same time, with the three value ranges of length EF types, there are 9 limit position points in total. Take points E_1, E_2, and E_3 on h_1, E_4, E_5, and E_6 on h_2, E_7, E_8, and E_9 on h_3, then the length F_1E_1 = F_1E_2 = F_1E_3 = 75.9mm, F_2E_4 = F_2E_5 = F_2E_6 = 85.1mm, F_3E_7 = F_3E_8 = F_3E_9 = 94.3mm, as shown in the figure 4. In this way, ankle shape is specifically divided into 27 groups.
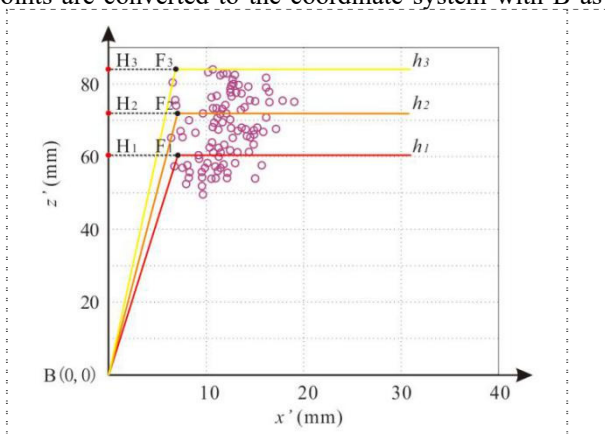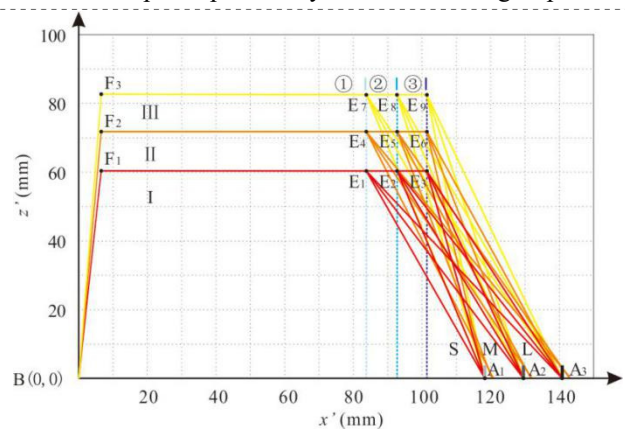

Figure 3. Distribution of point F.

Figure 4. Groups.

In fact, not all groups mentioned above exist, so we map 105 groups of data obtained from actual scanning to 27 groups, and observe the distribution of each group. As shown in the table 4, there are actually 17 groups. It can be seen from the actual groups that type III and type ③ in type S are absence, namely, there is no group with very small foot girth length, while ankle height and leg girth length are very large. This indicates that foot girth length is small, and ankle height and leg girth length are not too large. In type L, there may be various leg dimension and ankle height with large foot girth length. In type ③, only I(L)∪③, II(L)∪③, and III(L)∪③ exist, indicating that the leg dimension is large, and the

foot dimension must be large. In type ①, if the leg dimension is small, there may be various foot dimension types and ankle height. Nearly 16% of the small and short ones represented by groups I(S)∪① and I(S)∪② were mainly female, and 14% of the large and high ones represented by groups III(L)∪② and III(L)∪③ were male.

Table 4. Shape classification.

I(S)∪①	II(S)∪①	III(S)∪①	
M, F, P 0, 10, 9.5%	M, F, P 1, 3, 3.8%	NO	——

I(S)∪②	II(S)∪②	III(S)∪②
M, F, P 0, 7, 6.7%	M, F, P 0, 2, 1.9%	NO ——
I(S)∪③	II(S)∪③	III(S)∪③
NO ——	NO ——	NO ——
I(M)∪①	II(M)∪①	III(M)∪①
M, F, P 0, 5, 4.7%	M, F, P 2, 12, 13.3%	M, F, P 6,1, 6.7%
I(M)∪②	II(M)∪②	III(M)∪②
M, F, P 0, 4, 3.8%	M, F, P 3, 4, 6.7%	M, F, P 3, 0, 2.9%
I(M)∪③	II(M)∪③	III(M)∪③
NO ——	NO ——	NO ——
I(L)∪①	II(L)∪①	III(L)∪①
NO ——	M, F, P 0, 1, 1%	M, F, P 9, 2, 10.5%
I(L)∪②	II(L)∪②	III(L)∪②
NO ——	M, F, P 8, 1, 8.6%	M, F, P 12, 0, 11.4%
I(L)∪③	II(L)∪③	III(L)∪③
M, F, P 2, 0, 1.9%	M, F, P 3, 1, 3.8%	M, F, P 3, 0, 2.9%

3.4 Distribution of the medial and lateral ankle protrusion

We checked out the data of distance of the medial and lateral ankle protrusion (CD). The distribution of the values corresponding to the 17 groups mentioned above is shown in the table 5. In each specific group, the distribution span of CD is large. In terms of the overall distribution, the larger values of the corresponding EF, the greater of the overall CD_{mean} values in the same group divided by AB. For instance, CD_{mean} of I(S)∪① is 63.4mm, while CD_{mean} of I(S)∪② is 65.9mm. Similarly, in the same group divided by EF, the larger values the corresponding AB are, the greater overall CD_{mean} values will be. For example, the CD_{mean} of I(S)∪② is 65.9mm, while that of I(M)∪② is 69.2mm. That is to say, CD is affected by AB and EF simultaneously. Because the upper limit value of most product design parameters is considered, the maximum distance of CD in each group can be taken as a reference.

Table 5. The distribution of distance CD(mm).

Groups	CD_{min}	CD_{max}	CD_{mean}	Groups	CD_{min}	CD_{max}	CD_{mean}	Groups	CD_{min}	CD_{max}	CD_{mean}
I(S)∪①	58.4	69.6	63.4	II(S)∪①	60.6	70.0	67.1	III(S)∪①	\	\	\
I(S)∪②	62.2	70.6	65.9	II(S)∪②	68.5	73.2	70.8	III(S)∪②	\	\	\
I(S)∪③	\	\	\	II(S)∪③	\	\	\	III(S)∪③	\	\	\

I(M)∪①	63.4	71.6	66.9	II(M)∪①	63.6	73.7	67.4	III(M)∪①	67.8	78.8	70.7
I(M)∪②	66.6	71.3	69.2	II(M)∪②	64.5	76.1	70.4	III(M)∪②	71.5	75.6	73.7
I(M)∪③	\	\	\	II(M)∪③	\	\	\	III(M)∪③	\	\	\
I(L)∪①	\	\	\	II(L)∪①	66.6	66.6	66.6	III(L)∪①	65.7	75.6	71.5
I(L)∪②	\	\	\	II(L)∪②	70.0	77.7	73.4	III(L)∪②	70.8	77.1	73.6
I(L)∪③	69.5	81.7	75.6	II(L)∪③	73.9	81.3	78.1	III(L)∪③	74.0	77.2	75.8

4 Matching design and comfort evaluation of ankle brace

The products related to ankle, such as ankle braces, ankle boot, and boots, should be matched the ankle morphological changes and groups, so as to meet users' physiological needs. The rigid ankle brace mainly limits the ankle joint. The movement in the direction of extension and flexion needs to be flexible, and its shape design forms are various. But it cannot deviate from the ankle shape changes and varies dimensions. This study carries out design of living example, and tests its comfort through user experience evaluation.

4.1 Factors of rigid ankle brace fit design

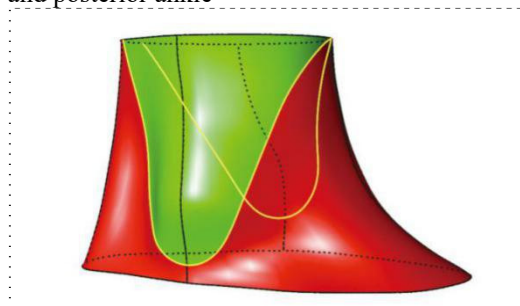(1) The brace design match to the morphological changes of anterior and posterior ankle

The design of a brace must give priority to the contraction and expansion deformations of anterior and posterior parts of the ankle. Through the calculation of the distance between two corresponding points on surface in each part, a boundary curve is obtained. This curve determined the specific deformed surface of skin. As shown in figure 5, the yellow curve divided the standard model into deformed skin surface (red) and non-deformed skin surface (green). The design of a brace should consider the deformed surface to match it.

(2) The brace design match to the asymmetry of medial and lateral ankle

As shown in figure 6, in standing state, we make surfaces AEK'J' and J'K'FB that are symmetric with parts AEKJ and JKFB along the plane ABEF. The differences in position between C and D' represented the asymmetry of medial and lateral ankle. They are the height difference of 10.1mm and anteroposterior difference of 11.3mm respectively.
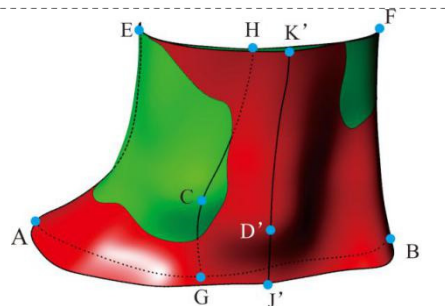

Figure 5. Area of deformed skin surface.

Figure 6. Surfaces AEK'J' and J'K'FB.

(3) The brace design match to the ankle groups

Wide ranges of ankle dimensions determine the product with the diversity of sizes. For ankle braces design, the purpose of meeting the comfort needs of mass users and matching the shape of products and ankle as much as possible. That is very important to combine the shape classification of ankle.

4.2 Rigid brace design

According to the specific usage and function of ankle brace, we design a rigid ankle brace according to the dimensions of group II(M) ∪ ① which has a large proportion of relative number of samples. The brace consists of the medial rigid part, the lateral rigid part, the foot area rigid part, the elastic material part, and the connecting fastener. The foot area rigid part and the elastic material part are taken as a whole. When the brace is used, the medial and the lateral rigid part are connected and fixed by connecting fastener. The appearance size of the brace should be set according to the thickness of rigid material and elastic material. Due to the change of ankle shape, the hollow part of the foot area between the medial and the lateral rigid part ensures the change of the extension and contraction of the ankle shape surface from 20° dorsiflexion to 50° plantar flexion. The foot size and classification are not discussed here. The parts and main dimensions are shown in the figure 7.
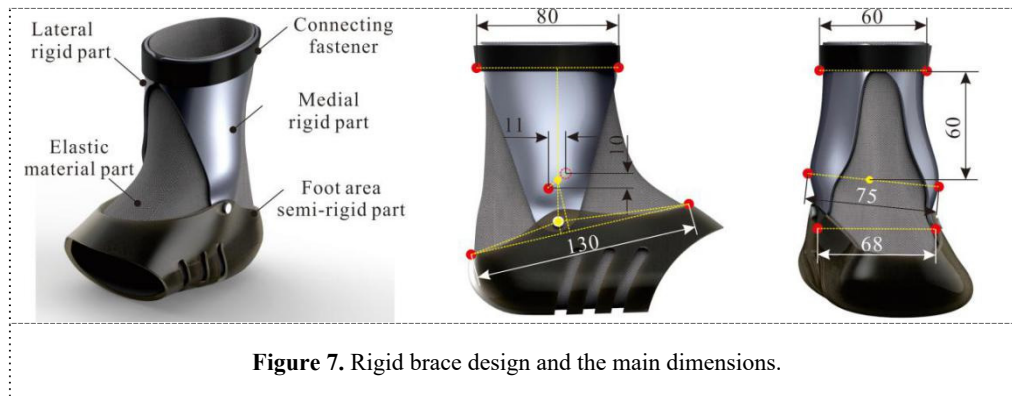
Figure 7. Rigid brace design and the main dimensions.

4.3 Comfort evaluation

Comfort is an important indicator of wearable products. The most intuitive evaluation method of comfort is subjective evaluation. In this study, we choose the proper users to wear the designed products of rapid prototyping, and then we evaluate the rigid ankle protection comfort in the following two ways through the user experience.

(1) Likert Scale

There are 10 subjects including 5 people with II(M) ∪① and 5 people with other groups of the ankle. Participants put on the designed braces according to the shape classification for more than 1 hour. Movement of walking, running or jumping can be allowed. We use the method of 5-order Likert Scale to judge the comfort effect based on the final score. There are 5 scores (1-5) for comfort, from low to high degree of comfort, and statistical results show that 5 people with II(M) ∪② of ankle are 21 scores in total, while people with other groups of ankle is 14 scores.

(2) Interview and comparison

Similarly, we look for 6 people with II(M)∪① of ankle, who wear designed product and a similar product on the market at the same time on both left and right feet. The two groups of products are randomly selected for the left and right foot, and the time is more than 1 hour. Do the same action as the first method. By way of inquiry, 4 of them feel that the designed braces has higher comfort degree, while 2 of them feel that there is not much difference between the two products.

5 Conclusions

The sample data with flexion and extension states of 105 legs and feet were scanned and unified the morphological model of the ankle. On this basis, (1) the feature of the ankle morphological changes was analyzed by dividing it into four parts. (2) The correlation analysis of ankle characteristic distances was made to establish 27 theoretical ankle shape groups. Through the analysis on data measured, there are actually 17 groups. (3) The percentage of samples in each of groups was counted, it showed that there were differences in ankle shape distribution between men and women, and the characteristic distance of female ankle shape was generally smaller than that of male. (4) The rigid brace design was taken as an example and the methods of

Likert Scale and interview were employed to evaluate the comfort of product design. The result showed that the method of design with the ankle morphological changes and shape groups was proved to be effective for matching the mass users.

Acknowledgments

References

1. Burdett, Ray, G. (1982) Forces predicted at the ankle during running. Medicine & Science in Sports & Exercise,14: 308-316.

2. Fong, D.T.P., Hong, Y., Chan, L.K., Yung, P.S.H., Chan, K.M. (2007) A Systematic Review on Ankle Injury and Ankle Sprain in Sports. Sports Medicine, 37: 73-94.

3. Abid, H., Mohd, J. (2019) 3D scanning applications in medical field: a literature-based review. Clinical Epidemiology and Global Health, 7: 199-210.

4. Claassen, L., Luedtke, P., Yao, D., Ettinger, S., Daniilidis, K., Nowakowski, A.M., Müller-Gerbl, M., Stukenborg-Colsman, C., Plaass, C. (2017) Ankle morphometry based on computerized tomography. Foot and Ankle Surgery, 23: 121.

5. Yu, J.F., Lee, K.C., Wang, R.H., Chen, Y.S., Fan, C.C., Peng, Y.C., Tu, T.H., Chen, C., Lin, K.Y. (2015) Anthropometry of external auditory canal by non-contactable measurement. Applied Ergonomics, 50: 50-55.

6. Harih, G., Dolsak, B. (2013) Tool-handle design based on a digital human hand model. International journal of industrial ergonomics, 43: 288-295.

7. Volonghi, P., Baronio, G., Signoroni, A. (2018) 3D scanning and geometry processing techniques for customised hand orthotics: an experimental assessment. Virtual and Physical Prototyping, 13: 1-12.

8. Ji, X.M., Zhu, Z.H., Gao, Z., Bai, X.B., Hu, G. (2018) Anthropometry and classification of auricular concha for the ergonomic design of earphones. Human Factors and Ergonomics in Manufacturing & Service Industries, 28: 90-99.

9. Sun, S.P., Chou, Y.J., Sue, C.C. (2009) Classification and mass production technique for three-quarter shoe insoles using non-weight-bearing plantar shapes. Applied Ergonomics, 40: 630-635.

10. Lee, Y.C., Wang, M.J. (2015) Taiwanese adult foot shape classification using 3D scanning data. Ergonomics, 58: 513-523.

11. Wang, C.S. (2010) An analysis and evaluation of fitness for shoe lasts and human feet. Computers in Industry, 61: 532-540.

12. Baek, S.Y., Lee, K. (2012) Parametric human body shape modeling framework for human-centered product design. Computer Aided Design, 44: 56-67.

13. Irzmańska, M., Okrasa, M. (2018) Evaluation of protective footwear fit for older workers (60+): a case study using 3D scanning technique. International Journal of Industrial Ergonomics, 67: 27-31.